

## A SIMPLE SYNTHESIS TECHNIQUE OF SINGLE-SQUARE-LOOP FREQUENCY SELECTIVE SURFACE

K. R. Jha<sup>1</sup>, G. Singh<sup>2, \*</sup>, and R. Jyoti<sup>3</sup>

<sup>1</sup>School of Electronics and Communication Engineering, Shri Mata Vaishno Devi University, Katra, Jammu and Kashmir 182301, India

<sup>2</sup>Department of Electronics and Communication Engineering, Jaypee University of Information Technology, Solan-173 234, India

<sup>3</sup>Space Application Center, Indian Space Research Organization, Ahmedabad, India

**Abstract**—In this manuscript, a simple synthesis method of single square loop frequency selective surface (SSLFSS) is discussed, which may find the suitable application in the fast analysis and fabrication of the frequency-selective surface. The presented technique is used to design SSLFSS at 3 GHz, 15 GHz, 22 GHz and 26 GHz. At every frequency of interest, the analytical result is very close to the required result. Moreover, a way to control the reflection at any frequency is discussed, which may find an application in controlling the reflection level at any frequency. However, we have proposed two simple, cheaper and lightweight structures at 3 GHz and 22 GHz for the application in various satellite communications. The proposed process has been extended to the analysis of bandpass structure and desired results have been achieved, which indicates the utility of the method of synthesis of both the bandpass and bandstop structures.

### 1. INTRODUCTION

Frequency selective surfaces (FSSs) are the periodic arrangement of conducting materials in one- or two-directions [1–3]. This kind of the structure finds numerous applications in microwave/millimeter wave and optical wave regime of the electromagnetic spectrum [4]. In the microwave and millimeter wave regime of the spectrum, FSS is used to improve the purity of the received signal, gain, directivity of an

---

*Received 1 September 2012, Accepted 19 October 2012, Scheduled 25 October 2012*

\* Corresponding author: Ghanshyam Singh (drghanshyam.singh@yahoo.com).

antenna, and Radom design etc. In the infrared and visible light wave regime of the spectrum, this kind of the structure is used as polarizer, beam splitter and in the solar energy collection, respectively [5, 6]. In the microwave and millimeter wave regime of the electromagnetic structure, the application of this kind of the structure is also noticeable in the satellite communication where it is required to maintain the purity of the signal in the specific band and to control the transmission and reflection of the signal to the desired level [7, 8].

To reduce the adjacent channel interference in the communication systems due to the congestion of the electromagnetic spectrum, several FSS structures like dipole, Jerusalem cross, ring, tripod, dross dipole and square loop have been developed [9]. It is noted that the square loop FSS (SLFSS) offers the better performance in terms of angular stability, cross polarization, bandwidth and band separation [1]. Due to these unique properties, single square loop frequency selective surface (SSLFSS) and double square loop frequency selective surface (DSLFFSS) have been investigated by several researchers [10–13]. Moreover, to analyze the FSS, various numerical techniques have been developed where each one is associated with its own merits and demerits [14]. Among these analytical techniques, equivalent circuit model is very popular due to its simplicity where the equivalent lumped parameters of a FSS is obtained due to the inductive and capacitive behavior of the loop arms and the gap between two loops. The analysis of FSS depends on the physical parameters like period ( $p$ ) of the loop, loop dimension ( $d$ ), width of the loop strip ( $w$ ) and gap between two loops ( $g$ ). In this proposed technique, after fixing the physical parameters, the value of associated inductance and capacitance are calculated to find the resonance, transmission and reflection conditions of the loop [15]. This model helps in finding resonance frequency of the structure, transmission, and reflection behavior of a loop when only the physical parameters are given. In another words, the existing literatures on the SSLFSS discusses about the analytical method but not its synthesis, which is very important to find the value of the physical parameter of the SSLFSS to meet the specific resonance frequency and bandwidth requirement.

In this contribution, a simple synthesis technique of a SSLFSS has been developed and a method to control the transmission and reflection level of the signal is discussed. The remainder of the manuscript is organized as follow. Section 2 deals the theory of operation of SSLFSS. In Section 3, the results obtained by the analytical solution and the numerical simulations are presented. Section 4 explores the effect of the incident angle on the FSS reflection property and in Section 5, a method to control the reflection coefficient is presented. In Section 6,

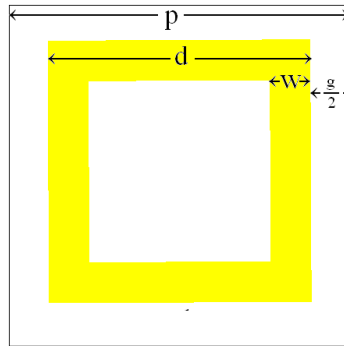


**Figure 1.** Single square loop FSS schematic.

the bandwidth control technique of a SSLFSS is discussed. In Section 7, two inexpensive FSS structure for Satellite communication system is proposed. In Section 8, the usefulness of the technique in the bandstop as well as bandpass FSS design has been explored and finally, the work is concluded in Section 9.

## 2. THEORY OF OPERATION

The equivalent circuit model of a SSLFSS is developed by [16] and this has been used to extract the circuit lumped parameters inductance ( $L$ ) and capacitance ( $C$ ) by several researchers [17,18]. With the help of the equivalent circuit model, the equivalent inductance and capacitance are obtained from the given physical parameters of an FSS like the periodicity ( $p$ ), loop length ( $d$ ), width of the strip ( $w$ ), angle of incidence ( $\theta$ ) and the inter-loop gap ( $g$ ), where these parameters are shown in Figure 1. However, in the design of an SSLFSS, it is desired to find the loop size and periodicity of the loop structure to resonate at the specific frequency and to have the desired bandwidth. The existing method only provides the knowledge about the value of the  $L$  and  $C$  for a given square loop but the accurate synthesis of the square loop from the knowledge of the resonance frequency is a challenging task and has not been dealt adequately. To overcome the synthesis difficulty of a SSLFSS, a simple and novel formula to calculate the loop dimension with certain accuracy has been developed.

For transverse electric (TE) polarized wave, the equivalent circuit elements are obtained by the following equations [10].

$$\frac{\omega_r L}{Z_0} = \frac{d}{p} \cos \theta \times F(p, w, \lambda, \theta) \quad (1)$$

$$F(p, w, \lambda, \theta) = \frac{p}{\lambda} \left[ \ln \csc \left( \frac{\pi w}{2p} \right) + G(p, w, \lambda, \theta) \right] \quad (2)$$

and

$$\frac{\omega_{rC}}{Y_0} = 4 \frac{d}{\lambda} \sec \theta \times F(p, g, \lambda, \theta) \cdot \varepsilon_{eff} \quad (3)$$

$$F(p, g, \lambda, \theta) = \frac{p}{\lambda} \left[ \ln \csc \left( \frac{\pi g}{2p} \right) + G(p, g, \lambda, \theta) \right] \quad (4)$$

In Equations (1)–(4),  $\varepsilon_{eff}$ ,  $Z_0$ ,  $Y_0$ ,  $G(p, w, \lambda, \theta)$ , and  $G(p, g, \lambda, \theta)$  are the effective dielectric permittivity of the media, characteristic impedance, characteristic admittance, the correction factors for the associated inductance and capacitance, respectively. When the correction factors are ignored at the cost of a minor deviation in the result, Equations (1) and (3) can be re-written as:

$$\frac{\omega_{rL}}{Z_0} = \frac{d}{p} \cos \theta \times \frac{p}{\lambda} \ln \left[ \csc \left( \frac{\pi w}{2p} \right) \right] \quad (5)$$

$$\frac{\omega_{rC}}{Y_0} = 4 \frac{d}{p} \sec \theta \times \frac{p}{\lambda} \ln \left[ \csc \left( \frac{\pi g}{2p} \right) \right] \times \varepsilon_{eff} \quad (6)$$

In the case of air as a substrate, the multiplication of Equations (5) and (6) gives:

$$\omega_r^2 LC = 4 \left( \frac{d}{p} \right)^2 \left( \frac{p}{\lambda} \right)^2 \times \ln \left[ \csc \left( \frac{\pi w}{2p} \right) + \csc \left( \frac{\pi g}{2p} \right) \right] \quad (7)$$

In Equation (7), the left-hand-side of the equation indicates the resonance/anti-resonance condition. For the reflective FSS, at the resonance, its value must be 1.0 because  $\omega_r^2 = 1/LC$ . Therefore, Equation (7) can be re-written in the following form.

$$1 = 4 \left( \frac{d}{p} \right)^2 \left( \frac{p}{\lambda} \right)^2 \times \ln \left[ \csc \left( \frac{\pi w}{2p} \right) + \csc \left( \frac{\pi g}{2p} \right) \right] \quad (8)$$

Further, Equation (8) is simplified as:

$$1 = 4 \left( \frac{d}{p} \right)^2 \left( \frac{p}{\lambda} \right)^2 \times \ln \left[ \frac{1}{\sin \left( \frac{\pi w}{2p} \right)} + \frac{1}{\sin \left( \frac{\pi g}{2p} \right)} \right] \quad (9)$$

For the case of  $w \ll 2p$  and  $g \ll 2p$ , Equation (9) is written as:

$$1 = 4 \left( \frac{d}{p} \right)^2 \left( \frac{p}{\lambda} \right)^2 \times \ln \left[ \frac{2p}{\pi w} + \frac{2p}{\pi g} \right] \quad (10)$$

In the case of the loosely packed FSS, the value of  $g$  is quite greater than  $w$  and the ratio of  $2p/\pi w$  dominates over the ratio of  $2p/\pi g$  and with the minor sacrifice in the accuracy, Equation (10) is simplified as:

$$1 = 4 \left( \frac{d}{\lambda} \right)^2 \times \ln \left( \frac{2p}{\pi w} \right) \quad (11)$$

It is known fact that for a given FSS structure, the response changes with the change in the angle of incidence of the wave and the period  $p$  of the FSS and to avoid the grating lobes, it is related to the wavelength ( $\lambda$ ) by the following relationship [19].

$$p(1 + \sin \theta) < \lambda \quad (12)$$

From Equation (12), it is observed that for a given maximum incident angle, a mathematical relation between  $p$  and  $\lambda$  may be established as long as the inequality is satisfied. To understand the concept, we take the case that the structure must operate satisfactorily over the angle  $\theta_1$ . Then we can select the value of  $\theta = \theta_2$  in Equation (12) where  $\theta_2 > \theta_1$ . On this way, it is revealed that the inequality of Equation (12) is satisfied and the value of  $p$  is fixed as:

$$p = M\lambda \quad (13)$$

In Equation (13),  $M$  is a constant and varies between 0 to 1. The substitution of Equation (13) in (11) gives the following expression.

$$1 = 4 \left( \frac{d}{\lambda} \right)^2 \times \ln \left( \frac{2M\lambda}{\pi w} \right) \quad (14)$$

From Equations (12) and (14), it is revealed that with the knowledge of the operating frequency, desired width of the strip as the fraction of wavelength, and maximum expected angle of the incident wave, the length of the loop may be calculated and further optimized. In general, the procedure is equally-suitable for the TM polarized wave. Since the square loop FSS is the polarization independent, the formula developed for the TE mode is also applicable to TM mode of operation. Further, this formula also provides a way to control the value of the reflection at any specific frequency. In Equation (7), the left hand side of the equation has been set as 1.0 for the resonance condition. Ideally, at this frequency, the value of  $|S_{11}|$  is equal to 1.0. If 1.0 in Equation (7) is replaced by some other value which is lesser than 1.0 then analysis shows the off-resonance condition and this may be used to govern the amount of the reflection at that particular frequency.

**Table 1.** Loop parameters at 3 GHz for  $10^\circ$  incident angle.

$w/\lambda$	$p$ (mm)	$d$ (mm)	$w$ (mm)	$f_r$ (GHz) (simulated)	% deviation of $f_r$ from 3 GHz
0.01	85.20	25.02	1	3.30	10
0.02	85.20	27.52	2	3.22	7.3
0.03	85.20	29.38	3	3.18	6
0.04	85.20	30.96	4	3.16	5.3
0.05	85.20	32.38	5	3.15	5.0
0.06	85.20	33.69	6	3.15	5.0

### 3. NUMERICAL RESULTS

To analyze the theory proposed in Section 2, the physical parameters of SSLFSS at 3 GHz, 15 GHz and 26 GHz have been computed and its correctness has been checked by the electromagnetic simulation in CST Microwave Studio, which based on the finite integral technique. In the first case, the loop parameters are analyzed for the normal incident wave ( $\theta = 0^\circ$ ). To calculate the value of  $p$  while avoiding grating lobe at the intended frequency, the value of  $p$  is calculated by meeting the condition described in Equation (12) and this condition which is for the analysis purpose and  $\theta > 0^\circ$  needs to be considered. In order to meet this synthesis constraint, the value of  $\theta = 10^\circ$  has been selected and on this way, the value of  $M$  is 0.1736. Once, the value of  $M$  is fixed, for the different value of  $w/\lambda$ , the value of  $d$  is calculated using the Equation (14) and it is presented in Tables 1, 2, and 3, for 3 GHz, 15 GHz, and 26 GHz, respectively. Further, to support the analysis, the structure has been simulated by CST Microwave Studio as shown in Figure 2. The value of the resonance frequency obtained by simulation is shown in 5th column of these Tables and in the last column, the relative error is shown.

These three tables show the various values of  $p$ ,  $d$ , and  $w$  at different frequencies for the normal incidence. However, the pattern of the Tables is similar. From these Tables, it is revealed that for the fixed value of  $p$ , with the increase in the value of  $w/\lambda$ , the relative percentage deviation from the intended frequency is reduced in spite of the normal incident of the electromagnetic wave as the structure has been simulated in the Transient Solver which supports the normal incident only. Further, the response is saturated and the effect of the increase in the width of the strip on the  $f_r$  (resonance frequency) is insignificant. The deviation is significantly reduced with the strip width but the small error still exists as in the simplified

**Table 2.** Loop parameters at 15 GHz for 10° incident angle.

$w/\lambda$	$p$ (mm)	$d$ (mm)	$w$ (mm)	$f_r$ (GHz) (simulated)	% deviation of $f_r$ from 15 GHz
0.01	17.04	5.00	0.2	16.56	10.4
0.02	17.04	5.50	0.4	16.09	7.2
0.03	17.04	5.87	0.6	15.91	6
0.04	17.04	6.19	0.8	15.81	5.4
0.05	17.04	6.47	1.0	15.75	5.0
0.06	17.04	6.73	1.2	15.75	5.0

**Table 3.** Loop parameters at 26 GHz for 10° incident angle.

$w/\lambda$	$p$ (mm)	$d$ (mm)	$w$ (mm)	$f_r$ (GHz) (simulated)	% deviation of $f_r$ from 26 GHz
0.01	9.83	2.88	0.11	28.65	10.1
0.02	9.83	3.17	0.23	27.92	7.3
0.03	9.83	3.39	0.34	27.56	6
0.04	9.83	3.57	0.46	27.40	5.3
0.05	9.83	3.73	0.57	27.32	5
0.06	9.83	3.88	0.69	27.13	4.3

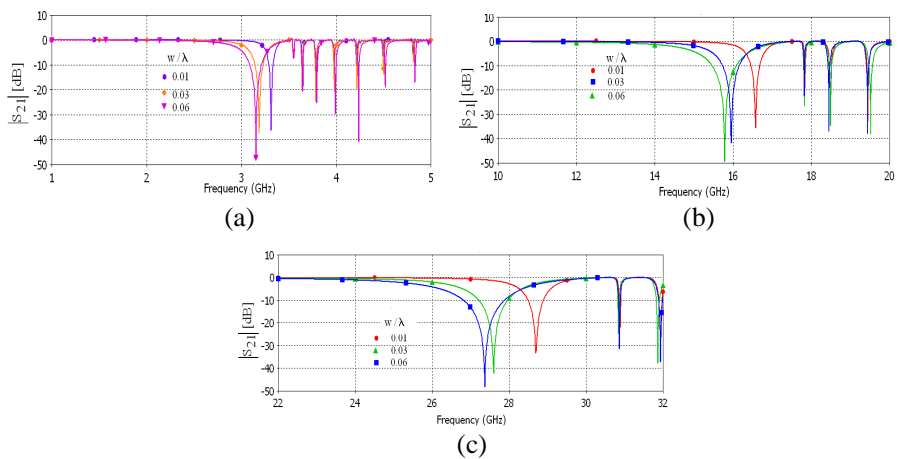


**Figure 2.** The effect of  $w/\lambda$  on the resonance frequency on (a) 1–5 GHz, (b) 12–18 GHz, and (c) 22–32 GHz range.

calculation, the value of the correction factor and the gap has been ignored. However, it is important to note that with the removal of the correction factor simplifies the synthesis process. The simulated value of the  $S_{21}$  parameter in 1–5 GHz, 10–20 GHz and 22–32 GHz are shown in Figure 2(a), Figure 2(b) and Figure 2(c), respectively which show different transmission zero points as mentioned in Tables 1, 2 and 3.

From Figures 2(a), (b) and (c), it is revealed that at a given incident angle ( $10^\circ$  in this case), with the increase in the  $w/\lambda$  ratio, the transmission zero point shifts to the lower frequency and the transmission zero bandwidth is increased. In the other words, with the increase in the value of the width of the strip, the inductive effect of the SSLFSS is reduced and it causes the width of the scattering parameter to increase. In the lossless condition,  $|S_{21}|^2 + |S_{11}|^2 = 1$  and it indicates that where  $S_{21}$  is minimum,  $S_{11}$  reaches to maximum and the flatness of the reflective property of the SSLFSS is increased. Further, from this analysis, it is clear that by changing the value of  $w/\lambda$ , the desired band of the rejection of the signal is achievable.

#### 4. EFFECT OF INCIDENT ANGLE

From Figures 2(a), (b) and (c), it is seen that the maximum relative error between intended and achieved operating frequency is about 10% which can be further reduced by reducing the value of  $\theta$  in Equation (12). When this value is set equal to zero, the value of  $p$  is equal to  $\lambda$  and Equation (12) is not satisfied which calls for the addition of the correction factor in the Marcuvitz Equation [16]. However, to design a loop, we set the angle  $\theta$  close to  $0^\circ$  for the normal incident wave and in this case the error is reduced significantly. To see this effect, the dimension of the SSLFSS at 3 GHz has been calculated for various value of the theta in the range of  $0^\circ$  to  $90^\circ$  as presented in Table 4. The structure has also been simulated for the normal incidence case in the transient solver of CST Microwave Studio and the resonant frequency has been observed which is shown in the last column of Table 4. To obtain the variation in the resonance frequency due to the change in the incident angle,  $w/\lambda$  ratio has been fixed to 0.06. It is observed from Table 4 that with the increase in the angle of incidence, the difference between expected resonance frequency and the simulated one with normal incidence increase first and then reduced. The maximum deviation is about 12% at  $40^\circ$ . Theoretically, with the increase in the angle of incidence, the value of  $p$  is reduced and the array becomes densely packed and at lower incidence angle the FSS array is loosely packed. On this way, it is seen that with the certain relaxation in the accuracy, the formula can be used for loosely as well as densely

**Table 4.** Effect of angle on a SSL FSS designed at 3 GHz with  $0.06w/\lambda$ .

Angle ( $\theta$ ) (degree)	$p$ (mm)	$d$ (mm)	$w$ (mm)	Simulated ' $f_r$ ' (GHz)
0	100	32.5346	6	2.87
5	91.9831	33.1259	6	3.03
10	85.2000	33.6969	6	3.15
15	79.4395	34.2461	6	3.23
20	74.8145	34.7721	6	3.30
25	70.2929	35.7475	6	3.32
30	66.6667	35.7475	6	3.33
35	63.5495	36.1932	6	3.35
40	60.8721	36.6083	6	3.36
45	58.5786	36.9911	6	3.32
50	56.6237	37.3396	6	3.32
55	54.9707	37.6520	6	3.30
60	53.5898	37.9265	6	3.27
65	52.4574	38.1617	6	3.24
70	51.5546	38.3562	6	3.21
75	50.8666	38.3562	6	3.18
80	50.3827	38.6183	6	3.17
85	50.0953	38.6844	6	3.15
90	50.0000	38.7065	6	3.14

packed FSS array. The effect of the variation in the angle of incidence on the normally incident simulation in the range of  $0^\circ \leq \theta \leq 60^\circ$  is shown in Figure 3. From Figure 3, it is revealed that at every incidence angle used in this calculation, except for  $\theta = 0^\circ$ , the SSLFSS resonates between 3 to 3.5 GHz and it shows the convergence of the result. In the case of  $\theta = 0^\circ$ , the resonance occurs at 2.87 GHz which is lower than the intended frequency (3 GHz) as it does not satisfy Equation (12). Further, from Figure 3, it is observed that with different value of the incident angle, the periodicity of the FSS, dimension of the loop and the width of the loop changes and it causes the shift in the resonance frequency and its bandwidth also. On this way, it helps in deciding about the bandwidth of the FSS. Further, to validate the theory, the result has been computed for 15 GHz and 26 GHz and the similar behavior has been observed. The observation in the range of  $30^\circ \leq \theta \leq 60^\circ$  is shown in Table 5 and Table 6, respectively.

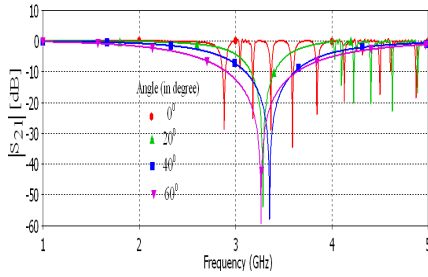


**Figure 3.** The effect of the angle of incidence on the  $S_{21}$  (magnitude in dB) parameter.

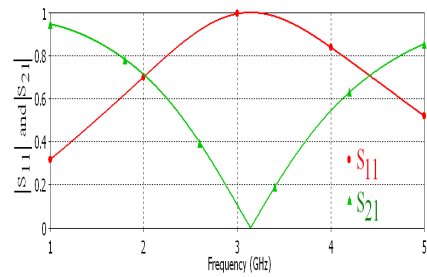


**Figure 4.** Scattering parameters of SSL FSS of loop length 38.7065 mm period, 50 mm, and width 6 mm at 3 GHz.

**Table 5.** Effect of angle on a SSL FSS designed at 15 GHz with  $0.06w/\lambda$ .

Angle (degree)	$p$ (mm)	$d$ (mm)	$w$ (mm)	Simulated ' $f_r$ ' (GHz)
30	13.3333	7.1495	1.2	16.7
35	12.7099	7.2386	1.2	16.83
40	12.1744	7.3217	1.2	16.82
45	11.7157	7.3982	1.2	16.78
50	11.3247	7.4679	1.2	16.68
55	10.9941	7.5304	1.2	16.56
60	10.7180	7.5853	1.2	16.41

**Table 6.** Effect of angle on a SSL FSS designed at 26 GHz with  $0.06w/\lambda$ .

Angle (degree)	$p$ (mm)	$d$ (mm)	$w$ (mm)	Simulated ' $f_r$ ' (GHz)
30	7.6923	4.1247	0.6923	29.137
35	7.3326	4.1761	0.6923	29.224
40	7.0237	4.2240	0.6923	29.229
45	6.7591	4.2682	0.6923	29.153
50	6.5335	4.3084	0.6923	28.990
55	6.3428	4.3445	0.6923	28.79
60	6.1834	4.3761	0.6923	28.42

### 5. CONTROLLING THE REFLECTION COEFFICIENT

In various applications, it is required to control the reflection coefficient to a desired level at a specific frequency. In general, there is no any direct method to calculate or anticipate about the dimension of the loop size which can satisfy the desired reflection coefficient condition. In this Section, we have developed a relationship between the  $S_{11}$  parameter and the resonance frequency and further have also shown that the desired level of the reflection coefficient can be obtained by simply manipulating the design of the loop. To understand the design method, we draw the  $S_{11}$  parameter of a loop operating at 3 GHz whose period ( $p$ ), loop size ( $d$ ), and ' $w/\lambda$ ' ratio are 50 mm, 38.7065 mm and 0.06, respectively. From Table 4 (last row), it is clear that it corresponds to  $90^\circ$  incident angle and resonates at 3.14 GHz. The scattering parameter of the FSS is shown in Figure 4.

From Figure 4, it is revealed that the structure resonates at 3.14 GHz and  $S_{11}$  is 0 dB at 3.14 GHz and in the range of 2.6 GHz to 3.7 GHz, the value of  $S_{21}$  is less than  $-10$  dB and it shows the strong reflection of the normally incident signal. On the linear scale, it is clear that the maximum reflection corresponds to  $S_{11} = 1$  at 3.14 GHz and this is equal to 100% reflection. Now, we assume a condition in which it is required to maintain the value of reflection coefficient  $< 100\%$  at 3.14 GHz. To obtain this value, the geometrical parameter of the loop must be changed. However, the amount of the change depends on the flatness of  $S_{11}$  curve and its roll-off factor. When  $p$  and  $d$  of the loop is increased and  $w$  of the strip is decreased, the stop bandwidth is reduced and  $S_{11}$  parameter falls sharply and it does not maintain the linearity. However, in the present case as shown in Figure 4, with the wider strip width, the change in the  $S_{11}$  parameter either side of the resonance frequency is linear and it indicates that for the wider strip width and smaller loop, a linear relationship between the  $|S_{11}|$  and the operating frequency exists and states that to reduce the reflection coefficient  $S_{11}$  to  $x\%$  at frequency  $f_r$ ,  $S_{11}$  must be multiplied by  $x/100$  and correspondingly:

$$|S_{21}| = \sqrt{1 - \left(\frac{x}{100}\right)^2} \quad \text{for } |S_{11}| = 1 \tag{15}$$

To explore the concept of linearly increase or decrease in the maximum reflection frequency point, we look at the fundamental relationship between impedance ( $Z$ ) and scattering ( $S$ ) parameters of the loop [20].

$$\begin{bmatrix} Z_{11} & Z_{12} \\ Z_{21} & Z_{22} \end{bmatrix} = Z_0 \begin{bmatrix} \frac{(1+S_{11})(1-S_{22})+S_{12}S_{21}}{(1-S_{11})(1-S_{22})-S_{12}S_{21}} & \frac{2S_{12}}{(1-S_{11})(1-S_{22})-S_{12}S_{21}} \\ \frac{2S_{21}}{(1-S_{11})(1-S_{22})-S_{12}S_{21}} & \frac{(1-S_{11})(1+S_{22})+S_{12}S_{21}}{(1-S_{11})(1-S_{22})-S_{12}S_{21}} \end{bmatrix} \tag{16}$$

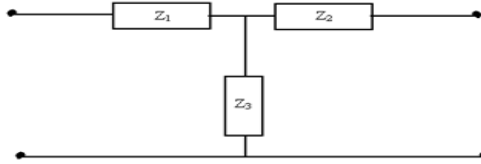


**Figure 5.** Equivalent circuit model of SSLFSS.

The  $Z$ -parameter is converted into its equivalent T-Network as shown in Figure 5 where  $Z_1$  and  $Z_2$  are equal to zero [15].

In Figure 5, the value of normalized impedance  $Z_3$  is related to the equivalent circuit model by the following formula.

$$Z_3 = j \left( \frac{\omega_r L}{Z_0} - \frac{Y_0}{\omega_r C} \right) \quad (17)$$

where  $Y_0 = 1/Z_0$  and  $L$  and  $C$  are equivalent inductance and capacitance at  $\omega_r$  as mentioned in Equations (5) and (6). From Equation (17), it is revealed that FSS impedance  $Z_3$  is directly proportional to the inductance and the operating frequency and inversely proportional to the capacitance. In the case of loosely packed FSS, the value of capacitance is negligible in comparison to the inductance. Under this condition,  $Z_3$  is proportional to  $\omega_r$ . It states that for loosely packed FSS, Scattering parameter is proportional to the impedance of FSS and the proportional change in the value of scattering parameter at the resonance frequency may be achieved by the change in the impedance level. To make this change, the resonance frequency of the loop must be increased by the same factor. On this way, a complete control on the scattering parameter is possible. For example, when we need the  $S_{11} = 10\%$  at 3 GHz, it indicates that the FSS corresponding to the resonance of 30 GHz to be designed as 3 GHz must be scaled up by 3 GHz/0.1. Further, to maintain the linearity of the curve, we select the design parameter as shown in the last row of Table 4 as the value at 3 GHz that is  $\theta = 90^\circ$  and  $p = 0.5\lambda$  from Equation (12). On this way, to achieve 10% reflection at 3 GHz, SSLFSS must be designed to resonate at 30 GHz. For the various values of the reflection levels, the outcome of this process to control the reflection is shown in Table 7.

From the first and the last column of Table 7, it is clear that for the wider strip and loosely packed SSLFSS, the required value of the reflection is achievable by simply scaling up the resonance frequency by that factor. Further, the first significant figure of the last column is very close to the required magnitude of the reflection coefficient. The simulated result of  $|S_{11}|$  against the frequency is shown in Figure 6.

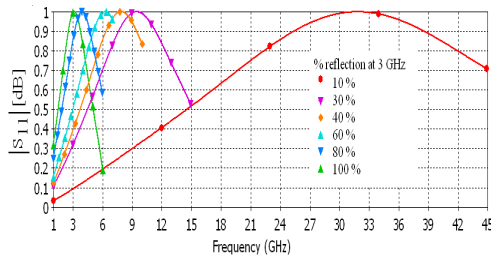


**Figure 6.** Controlled reflection coefficient at 3 GHz.

**Table 7.** Controlling the reflection coefficient by varying the loop size.

Required $S_{11}$ at 3 GHz	SSL FSS designed to resonate at	The loop parameter for $w/\lambda = 0.06$				Simulated value of $S_{11}$ at 3 GHz (in fraction)
		$\lambda$ (mm)	$P$ (mm)	$d$ (mm)	$w$ (mm)	
0.1	30 GHz	10	5	3.8706	0.6	0.0971
0.2	15 GHz	20	10	7.7413	1.2	0.1963
0.3	10 GHz	30	15	11.6119	1.8	0.3325
0.4	7.5 GHz	40	20	15.4826	2.4	0.4078
0.5	6 GHz	50	25	19.3532	3	0.5223
0.6	5 GHz	60	30	23.2239	3.6	0.6443
0.7	4.28 GHz	70.09	35.04	27.1307	4.2	0.7696
0.8	3.75 GHz	80	40	30.9652	4.8	0.8823
0.9	3.33 GHz	90.09	45.04	34.8707	5.4	0.9658
1.0	3 GHz	100	50	38.7065	6	0.9993

From Figure 6, it is clear that the resonance frequency obtained for the different geometrical parameters of the loop as mentioned in column 5, 6, and 7 of Table 7 is in the agreement to the required resonance frequency as described in column 2 of Table 7. Since, the resonance conditioned is satisfied,  $|S_{11}|$  is also satisfied at 3 GHz.

Further, to validate the proposed method of analysis of the reflection coefficient at a given frequency, the procedure has been repeated at 15 GHz and similar result has been obtained. The required geometrical parameter to achieve the desired reflection coefficient at 15 GHz is shown in Table 8 and in the last column, the value of the achieved reflection coefficient at 15 GHz is shown. Further, the structures have been simulated in the 12–18 GHz frequency window as shown in Figure 7 and the observed reflection coefficient at 15 GHz is comparable to the desired one. On this way, it is concluded that to

achieve the desired reflection co-efficient at any frequency, the frequency is to be divided by that fraction of the reflection coefficient and the new frequency serves as the resonance frequency of the structure.

## 6. BANDWIDTH CONTROL

The band of operation of SSLFSS is largely affected by the loop size and the width of the loop strip. When the size of the loop is reduced and strip width is increased, the rejection bandwidth of FSS is also increased and with the enhancement in the loop size, the bandwidth is decreased. It indicates that the bandwidth is inversely related to

**Table 8.** Controlling the reflection coefficient by varying the loop size at 15 GHz.

Required $S_{11}$ at 15 GHz	SSL FSS designed to resonate at	The loop parameter for $w/\lambda = 0.06$				Simulated value of $S_{11}$ at 15 GHz (in fraction)
		$\lambda$ (mm)	$P$ (mm)	$d$ (mm)	$w$ (mm)	
0.1	150 GHz	2	1	0.77	0.12	0.104
0.2	75 GHz	4	2	1.54	0.24	0.200
0.3	50 GHz	6	3	2.32	0.36	0.298
0.4	37.5 GHz	8	4	3.09	0.48	0.403
0.5	30 GHz	10	5	3.87	0.60	0.511
0.6	25 GHz	12	6	4.64	0.72	0.621
0.7	21.43 GHz	13.98	6.99	5.41	0.83	0.745
0.8	18.75 GHz	16	8	6.19	0.96	0.855
0.9	16.66 GHz	17.98	8.99	6.96	1.08	0.944
1.0	15 GHz	20	10	7.74	1.2	0.993

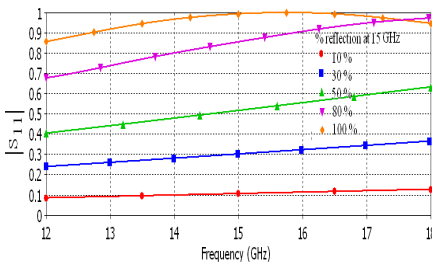


**Figure 7.** The value of controlled reflection coefficient in the range of 12–18 GHz.

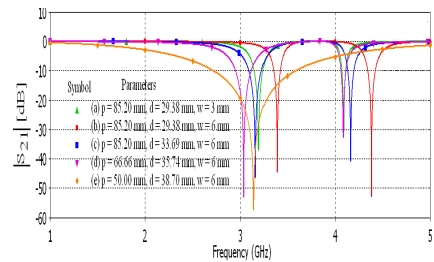


**Figure 8.** Effect of the loop parameters on the  $|S_{21}|$  parameter.

the  $d$  and  $p$ . Even though in the case of larger loop, the bandwidth may further be controlled by the variation in the  $w$ . To show, the effect of the loop size and its strip width on the transmission/reflection bandwidth of SSLFSS, we have analyzed five structures with different parameters at 3 GHz as: a)  $p = 85.20$  mm,  $d = 29.38$  mm,  $w = 3$  mm, b)  $p = 85.20$  mm,  $d = 29.38$  mm,  $w = 6$  mm, c)  $p = 85.20$  mm,  $d = 33.69$  mm,  $w = 6$  mm, d)  $p = 66.6667$  mm,  $d = 35.7475$  mm,  $w = 6$  mm, and e)  $p = 50$  mm,  $d = 38.7065$  mm, and  $w = 6$  mm where parameters mentioned in (a) and (c) are taken from Table 1 and (d) and (e) from Table 4. The  $S_{21}$  parameter of the structures is shown in Figure 8. From Figure 8, it is revealed that, for the case (a) and (b) and (c) where the periodicity is close to the wavelength, the rejection bandwidth is narrow. Further, in the case (a) strip width is 3 mm in comparison to (b) where the strip width is equal to 6 mm. Due to the change in only the strip width the resonance frequency shifts to 3.24 GHz from 3.14 GHz in the case of (a). The half power bandwidth in the case of (a) and (b) are 7.64% and 5%, respectively. It indicates that for the narrow bandwidth, the strip width is to be increased but the structure resonates at higher frequency. Now in the case (c), while keeping the same  $p$  and  $w$  as of (b), and increasing the value of  $d$ , the resonance frequency shifts downward and it is due to the reduction in the quality factor which has been reduced due to the change in the inductance value where inductance is associated with the strip width. In the case (c), the  $f_r$  and  $-3$  dB fractional bandwidth (FBW) are 3.11 GHz and 8.66%, respectively. In the case of (d) and (e), the periodicity  $p$  and loop dimension  $d$  have been reduced and increased, respectively, while keeping the strip width constant equal to 6 mm. With the reduction in the periodicity, the rejection bandwidth is increased which is evident from Figure 8. On this way, the smaller size loop may be used to increase the band-rejection limit which would be a wide band rejection. Another important phenomenon is the effect of the  $p$  on the resonance condition of the structure. If the periodicity is close to the wavelength, multiple resonances is achieved and may be used in the design on multi-resonance FSS structure [13] and for the wide band rejection smaller loop is required.

## 7. DESIGN OF A LOW COST INEXPENSIVE SSLFSS FOR SATELLITE COMMUNICATION

In the preceding sections, the SSLFSS has been analyzed in detail without any dielectric support to the structure. However, for the practical purpose, it is necessary to design the FSS on a dielectric material. However, the use of the dielectric material changes the

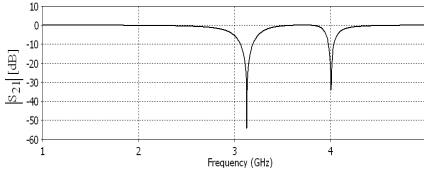


**Figure 9.** The transmission property of FSS with Thermocol dielectric support.

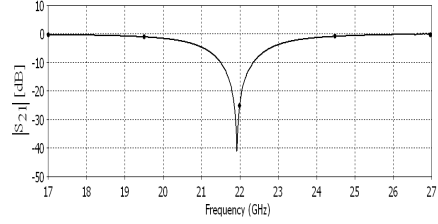


**Figure 10.** The transmission response of FSS at 22 GHz.

performance of the structure [21] as the characteristic impedance above and below the structure is changed and operating frequency shifts downward with proportion of  $\varepsilon_{eff}^{-1/2}$  [1, 2]. It indicates that the low-relative dielectric permittivity material is a good choice of substrate in the FSS design. In view of this fact, we consider a dielectric support of Thermocol whose relative dielectric permittivity is 1.05. The selection of this kind of material reduces the separate analytical treatment of the structure as its relative dielectric permittivity is close to the free-space and the dependence of the performance of the FSS on the substrate is alleviated. The independence of the performance to the substrate thickness leads to enhance the mechanical strength of the structure by the selection of thicker substrate. Keeping these facts in mind, two FSS structures at 3 GHz and 22 GHz with about 10% bandwidth for the satellite communication is designed. The structure is similar to the structure shown in Figure 1 except at the back side of a dielectric support of Thermocol of relative dielectric permittivity 1.05 of thickness 10 mm is placed. The dimension of the structure has been parametrically tuned to resonate near 3 GHz and in this case  $p$ ,  $d$ ,  $w$ , and FSS conductor thickness ( $t$ ) are 85.20 mm, 33.69 mm, 6 mm and 0.01 mm, respectively. The response of structure is shown in Figure 9 where it is noted that the structure resonates at 3.1 GHz and the FBW bandwidth is 9.2%.

From Table 2 and Table 3, it is observed that with the increase in the operating frequency, for narrow strip width and longer period, the bandwidth narrows but relative error is increased and it is quite significant where the precise application of the spectrum is needed. To overcome this constraint, we have designed a structure with  $f_r = 20$  GHz,  $w/\lambda = 0.02$ ,  $\theta = 20^\circ$  and correspondingly  $p$ ,  $d$  and  $w$  are 11.1772 mm, 4.21149 mm and 0.3 mm, respectively. The conducting material and substrate thickness are 0.01 mm and 10 mm, respectively.

The response of the structure is shown in Figure 10 and from this figure, it is revealed that the FBW is 10.9% and the structure resonates at 21.96 GHz which is in close agreement to the requirement.

## 8. EXTENSION OF THE PROCEDURE TO BANDPASS FSS DESIGN

It is known fact that the bandpass and bandstop FSS are complementary to each other. Due to this nature of the structure, a bandstop FSS structure can be converted into bandpass by replacing the conducting material part by the slot and the vacant part of the FSS by the conductor. In this case, the period  $p$  remains same and the width  $w$  is replaced by the slot width and  $d$  becomes the length of the slot. It indicates that the synthesis process developed in this work is also suitable to find the parameters of the square shape bandpass FSS. To see the process of the analysis of the bandpass response, we have designed bandstop and bandpass FSS in two different frequency bands. In the first case, the value of  $p$ ,  $d$ , and  $w/s$  are 50 mm, 38.70 mm, and 6 mm, respectively. The parameter values are shown in the last line of Table 4 and expected resonance frequency in bandpass as well as in the bandstop FSS structure is 3.14 GHz. The bandstop and bandpass FSS to resonate at this frequency is shown in Figures 11 (a) and (b) respectively.

The simulated frequency response of the structures shown in Figures 11(a) and (b) are shown in Figures 12(a) and (b), respectively. The comparison of two figures clearly reveals that the resonance frequency in both the cases is same and it is 3.14 GHz. The only

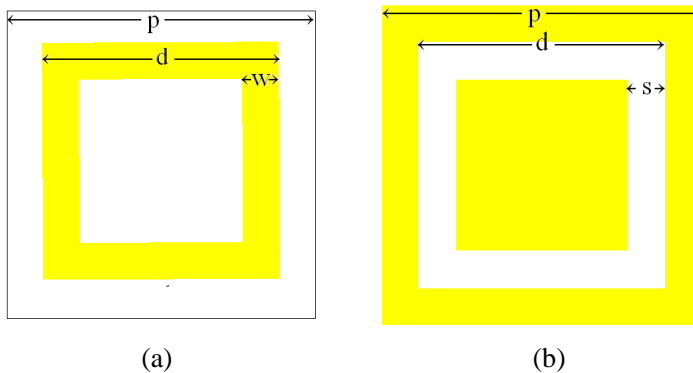


**Figure 11.** Frequency selective surface, (a) bandstop and (b) bandpass.

difference is the interchange of  $S_{21}$  and  $S_{11}$  parameter and it indicates that the both bandpass and bandstop FSS can be realized with this technique.

To verify the consistency of the approach, the similar structure as shown in Figures 11(a) and (b) have been simulated at 22–30 GHz frequency band for narrow slot and strip width. The FSS parameters are  $p = 9.83$  mm,  $d = 3.39$  mm and  $w/s = 0.34$  mm, respectively. The structure parameters are taken from the 3rd line of the Table 3. The structures are shown in Figures 12(a) and (b), respectively.

The response of the structures shown in Figures 13(a) and (b) are shown in Figures 14(a) and (b), respectively. From the analysis of the frequency responses, it is revealed that both the structures resonate near 27.5 GHz and they have similar graph pattern except the interchange in the  $S_{11}$  and  $S_{21}$  parameters.

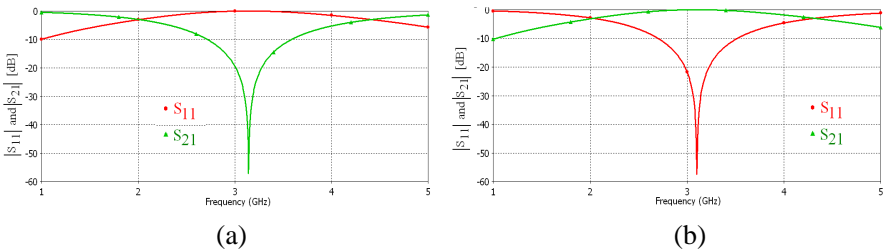


**Figure 12.** The response of the (a) bandstop and (b) bandpass FSS in 1–5 GHz band.

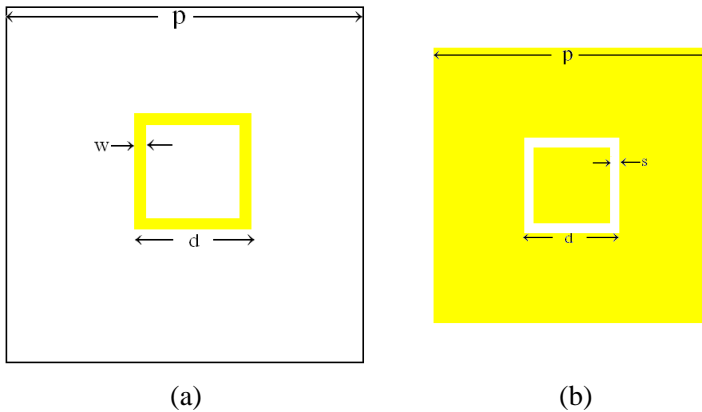


**Figure 13.** The frequency selective surface, (a) bandstop and (b) bandpass at 22–30 GHz range.

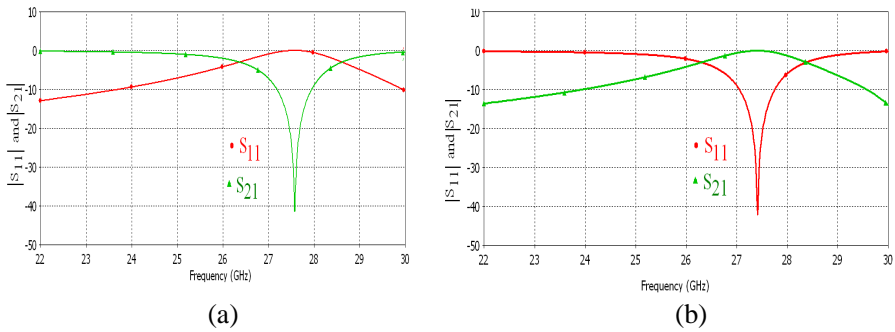


**Figure 14.** The response of the (a) bandstop and (b) bandpass FSS at 22–30 GHz band.

## 9. CONCLUSION

In this paper, a simple synthesis technique of SSLFSS is proposed. The process of the calculation of various parameters is presented and the numerical technique has been supported by the simulation. In addition to this, the method to control the reflection at any frequency is also explored and it may find the application in interference control. Further, this method has been used to design two FSS structures at 3 GHz and 22 GHz with the controlled bandwidth which may find the suitable application in satellite communication. Moreover, the process has been extended to the synthesis of bandpass FSS structure and the desired results have been obtained which indicates the application of the process for both types of the FSS. However, the angular sensitivity of the structure for narrow bandwidth has not been discussed, which will be reported in future communications.

## ACKNOWLEDGMENT

This work is supported by the Indian Space Research Organization vide Project No. ISRO/RES/4/579/10-11.

## REFERENCES

1. Wu, T. K., *Frequency Selective Surfaces and Grid Array*, John Wiley and Sons, New York, 1995.
2. Munk, B. A., *Frequency Selective Surfaces: Theory and Design*, John Wiley and Sons, New York, 2000.

3. Sakran, F. and Y. Neve-Oz, "Absorbing frequency-selective-surface for the mm-wave range," *IEEE Trans. Antennas Propag.*, Vol. 56, No. 8, 2649–2655, 2008.
4. Singh, D., A. Kumar, S. Meena, and V. Agrawal, "Analysis of frequency selective surfaces for radar absorbing materials," *Progress In Electromagnetics Research B*, Vol. 38, 297–314, 2012.
5. Ulrich, R., "Far-infrared properties of metallic mesh and its complementary structure," *Infrared Physics*, Vol. 7, No. 1, 37–50, 1967.
6. Durschlag, M. S. and T. A. Detemple, "Far-IR optical properties of freestanding and dielectrically backed metal meshes," *Applied Optics*, Vol. 20, No. 7, 1245–1253, 1981.
7. Monni, S., A. Neto, G. Gerini, F. Nennie, and A. Tijhuis, "Frequency-selective surface to prevent interference between radar and SATCOM antennas," *IEEE Antennas Wireless Propag. Lett.*, Vol. 8, 220–223, 2009.
8. Rahmat-Samii, Y. and A. Densmore, "A history of reflector antenna development: Past, present and future," *Proc. IEEE Microwave and Optoelectronics Conference*, 17–23, California, USA, Nov. 3–6, 2009.
9. Bayatpur, F., "Metamaterial-inspired frequency-selective surfaces," Ph.D. Dissertation, University of Michigan, USA, 2009.
10. Yilmaz, A. E. and M. Kuzuoglu, "Design of the square loop frequency selective surfaces with particle swarm optimization via the equivalent circuit model," *Radioengineering*, Vol. 18, No. 2, 95–102, 2009.
11. Baytpur, F. and K. Sarabandi, "Single-layered high-order miniaturized-element frequency-selective surfaces," *IEEE Trans. Microw. Theo. Tech.*, Vol. 56, No. 4, 774–781, 2008.
12. Dickie, R., R. Cahill, H. Gamble, V. Fusco, M. Henery, M. Oldfield, P. Huggard, P. Howard, N. Grant, Y. Munro, and P. de Maagt, "Sub-millimeter wave frequency selective surface with polarization independent spectral responses," *IEEE Trans. Antennas Propag.*, Vol. 57, No. 7, 1985–1994, 2009.
13. Pirahadi, A., F. Keshmiri, M. Hakkak, and M. Tayarani, "Analysis and design of dual band high directivity EBG resonator antenna using square loop FSS as superstrate layer," *Progress In Electromagnetics Research*, Vol. 70, 1–20, 2007.
14. Mittra, R., C. H. Chan, and T. Cwik, "Techniques for analyzing frequency selective surfaces a review," *Proc. IEEE.*, Vol. 76, No. 12, 1593–1615, 1988.

15. Sung, H. H., "Frequency selective wallpaper for mitigating indoor wireless interference," Ph.D. Thesis, Auckland University, NZ, 2006.
16. Marcuwitz, N., *Waveguide Handbook*, McGraw-Hill, 1st Edition, New York, 1951.
17. Langley, R. J. and E. A. Parker, "Equivalent circuit model for arrays of square loops," *Electronics Letters*, Vol. 18, No. 7, 294–296, 1982.
18. Lee, C. K. and R. J. Langley, "Equivalent-circuit models for frequency selective surfaces at oblique angles of incidence," *IEE Proceedings H — Microwaves Optics and Antennas*, Vol. 132, 395–399, 1985.
19. Reed, J. A., "Frequency selective surfaces with multiple periodic elements," Ph.D. Dissertation, University of Texas at Dallas, USA, 1997.
20. Pozar, D. M., *Microwave Engineering*, 2nd Edition, John Wiley and Sons, NY, USA, 1998.
21. Callaghan, P., E. A. Parker, and R. J. Langley, "Influence of supporting dielectric layers on the transmission properties of frequency selective surfaces," *IEE Proc. H — Microwave Antennas Propagation*, Vol. 138, No. 5, 448–454, 1991.